

Article

Finite-Size Effects with Boundary Conditions on Bose-Einstein Condensation

Run Cheng ^{1,2}, Qian-Yi Wang ¹, Yong-Long Wang ^{2,*} and Hong-Shi Zong ^{1,3,4,*}

¹ Department of Physics, Nanjing University, Nanjing 210093, China; dg20220011@smail.nju.edu.cn (R.C.); mg1922031@smail.nju.edu.cn (Q.-Y.W.)

² School of Physics and Electronic Engineering, Linyi University, Linyi 276005, China

³ Joint Center for Particle, Nuclear Physics and Cosmology, Nanjing 210093, China

⁴ Department of Physics, Anhui Normal University, Wuhu 241000, China

* Correspondence: wangyonglong@lyu.edu.cn (Y.-L.W.); zonghs@nju.edu.cn (H.-S.Z.)

Abstract: We investigate the statistical distribution for ideal Bose gases with constant particle density in the 3D box of volume $V = L^3$. By changing linear size L and imposing different boundary conditions on the system, we present a numerical analysis on the characteristic temperature and condensate fraction and find that a smaller linear size is efficient to increase the characteristic temperature and condensate fraction. Moreover, there is a singularity under the antiperiodic boundary condition.

Keywords: finite-size effects; boundary conditions; Bose–Einstein condensation



Citation: Cheng, R.; Wang, Q.-Y.; Wang, Y.-L.; Zong, H.-S. Finite-Size Effects with Boundary Conditions on Bose-Einstein Condensation. *Symmetry* **2021**, *13*, 300. <https://doi.org/10.3390/sym13020300>

Academic Editors: Sergei D. Odintsov and Vladimir V. Konotop
Received: 21 December 2020
Accepted: 3 February 2021
Published: 10 February 2021

Publisher's Note: MDPI stays neutral with regard to jurisdictional claims in published maps and institutional affiliations.



Copyright: © 2021 by the authors. Licensee MDPI, Basel, Switzerland. This article is an open access article distributed under the terms and conditions of the Creative Commons Attribution (CC BY) license (<https://creativecommons.org/licenses/by/4.0/>).

1. Introduction

The Bose–Einstein condensation (BEC) is a purely quantum-statistical phase transition characterized by the appearance of macroscopic population in ground state below the critical temperature T_c , and it plays an important role in condensed matter [1–9], optics [10,11], atomic and molecular physics [12–15], etc. It is emphasized that the transition actually occurs at the thermodynamic limit, or when the discrete level structure is approximated by a continuous density of states [14,16–21].

However, the experimental observations of BEC on cold gases [16,17,19,22–28] were performed in the finite volume that neither of the above approximations methods seems to inherently justify [18,29]. Subsequently, some scholars wondered whether this would lead to deviations from the theoretical predictions and began to pay attention to BEC in finite systems [18,29–31]. The boundary conditions are of great importance to finite systems, such as periodic, Neumann, and Dirichlet conditions [29,30,32–36]. The results imply that the shift of the condensation temperature depends only on the total number of particles [18,29].

From the theoretical point of view, the only requirement is that the Hamiltonian of the finite system should be Hermitian, and the above boundary conditions are just some special cases. These inspire us to explore the physics of BEC in finite volume systems by focusing on the finite-size behaviors and twisted boundary conditions [37]. For simplicity, in this paper, we model the finite system with a 3D box of volume $V = L^3$ that consists of ideal Bose gases, keeping particle density fixed. We characterize BEC phase transition with characteristic temperature and condensate fraction, and then numerically calculate them under different linear sizes and boundary conditions.

This paper is organized as follows. In Section 2, the specific formulas for the statistical distribution of ideal Bose gases are directly given. In Section 3, through numerical calculations, finite-size effects on characteristic temperature and condensate fraction are investigated. In Section 4, the changes on characteristic temperature and condensate fraction are also obtained in the presence of twisted boundary conditions. Finally, in Section 5, conclusions and discussions are briefly given.

2. The Ideal Bose Gases in the Cubic Box

In this section, the BEC statistics of ideal Bose gases with fixed particle density n , which is confined in the cubic box of volume $V = L^3$, are directly given. According to the Bose–Einstein distribution, the population $N(\epsilon_i)$ of a state with energy ϵ_i is

$$N(\epsilon_i) = \frac{1}{e^{\beta(\epsilon_i - \mu)} - 1} = \frac{ze^{-\beta\epsilon_i}}{1 - ze^{-\beta\epsilon_i}} \tag{1}$$

and the particle density n is

$$n = \frac{1}{V} \sum_i \frac{1}{e^{\beta(\epsilon_i - \mu)} - 1} = \frac{1}{V} \sum_i \frac{ze^{-\beta\epsilon_i}}{1 - ze^{-\beta\epsilon_i}}, \tag{2}$$

where $\beta = 1/(k_B T)$ and k_B denotes the Boltzmann’s constant. The fugacity z related to chemical potential μ can be expressed by $z = \exp(\beta\mu)$. By splitting off the ground-state particle density n_0 , the finite sum over the excited states n_ϵ is replaced by an integral:

$$n_\epsilon = n - n_0 = \frac{1}{V} \sum_{j=1}^{\infty} z^j \int_{\epsilon}^{\infty} D(\epsilon) \exp(-j\beta\epsilon) d\epsilon, \tag{3}$$

where $n_0 = \frac{ze^{-\beta\epsilon_0}}{1 - ze^{-\beta\epsilon_0}}$. $D(\epsilon)$ represents the density of states, usually taken to be $\frac{2\pi V}{h^3} (2m)^{\frac{3}{2}} \epsilon^{\frac{1}{2}}$. h and m denote the Planck constant and the mass of boson, respectively. Assuming the ground state ϵ_0 as zero, the result is:

$$\frac{1}{V} \frac{z}{1 - z} + \frac{1}{\lambda^3} g_{3/2}(z) = n, \tag{4}$$

with $\lambda = \frac{h}{(2\pi mk_B T)^{1/2}}$ and the Bose function $g_n(z) = \sum_{m=1}^{\infty} z^m / m^n$. The physical meaning of the second term in Equation (4) implies that, as the fugacity z reaches its maximum $\exp(\beta\epsilon_0)$, the number of the excited particles reaches the maximum, and all particles that exceeding this maximum must drop into the ground state. Namely, the critical temperature T_c can now be found by setting $n_0 = 0$ and $z = 1$ as:

$$\frac{2\pi}{h^3} (2m)^{\frac{3}{2}} \int_0^{\infty} \frac{\epsilon^{\frac{1}{2}} d\epsilon}{e^{\frac{\epsilon}{k_B T_c}} - 1} = n. \tag{5}$$

We now consider the extension of an ordinary BEC, by confining ideal Bose gases into a finite cubic box with linear size L . For finite volume systems, it is always crossover rather than phase transition. We thus define characteristic temperature [36] $T_{c,L}$ of the finite system with linear size L by:

$$\frac{1}{V} \sum_i \frac{1}{z_0^{-1} e^{\epsilon_i / k_B T_{c,L}} - 1} = n, \quad (i = 1, 2, \dots) \tag{6}$$

with $z_0 = \exp(\epsilon_0 / k_B T_{c,L})$. This temperature becomes the critical temperature only in the limit when system size goes to infinity. Additionally, as for small systems, boundary conditions are of crucial importance as they can affect the symmetries of the system and consequently modify the fundamental properties, such as ground state energies and conserved quantities [38]. The components of energy and momentum are quantized when particular physical boundary conditions are imposed on the finite system, and the discussions of BEC statistics should use summation instead of integral.

For simplicity, we consider particles confined in a 3D cubic box of dimensions $L_x, L_y, L_z \in [-\frac{L}{2}, \text{ and } \frac{L}{2}]$. Theoretically, to ensure the momentum operators \hat{p}_x, \hat{p}_y , and \hat{p}_z in the

systems are Hermitian, the quantum probability density $\rho = |\psi|^2$ should be constant on the boundary of the cubic box. Namely,

$$\rho(x, y, z = -L/2) = \rho(x, y, z = L/2). \quad (7)$$

Therefore, the arbitrary wave function should meet $\psi_k(\frac{L}{2})/\psi_k(-\frac{L}{2}) = e^{i\alpha}$. These twisted boundary conditions are parameterized by a twist angle α at each boundary, with range $0 \leq \alpha \leq 2\pi$. The use of twisted boundary conditions for the BEC in the cubic box, which is equivalent to realizing the BEC in the presence of a constant background magnetic potential coupled with bosons. The twist angles characterizing the twisted boundary condition are only obtained at the discrete values of the eigenstates energies, which corresponds to the magnetic flux quanta $N\phi$. The stronger is the magnetic potential, the larger is the twisted angle. Especially, the discrete twist angles are related to the linear size L , energy levels are shifted, and finite-volume corrections can be generated [39]. Experimentally, according to the superfluid behavior of a BEC [40,41], the achievement of BEC in the cubic of side length L characterized with twisted boundary conditions may be realized in terms of the non-classical response of the system to an infinitesimal boost or rotation. The boost can be provided by imposing extremely small velocity field such as slow rotation of the cubic box, and the rotation can be equivalently produced by introducing disclinations and screw dislocations [42]. Therefore, the allowed components of particle's momenta inside the box are $p_{x,y,z} = \frac{2\pi}{L}N + \frac{\alpha}{L}$, where N is an integer. The corresponding energy eigenvalues of bosons in the cubic box are expressed as [43,44]:

$$\epsilon_{n_1 n_2 n_3} = \frac{\hbar^2 [(2n_1\pi + \alpha)^2 + (2n_2\pi + \alpha)^2 + (2n_3\pi + \alpha)^2]}{2mL^2}, \quad (8)$$

where the quantum states are characterized by the quantum numbers (n_1, n_2, n_3) , $(n_1, n_2, n_3 = 0, \pm 1, \pm 2, \dots)$. Consequently, we can absorb the effect of α into twist boundary conditions for the wavefunctions, to study different physical boundary conditions [45] on BEC in finite volume systems. Substituting Equation (8) into Equation (6), with the volume $V = L^3$, results:

$$\frac{1}{L^3} \sum_{n_1} \sum_{n_2} \sum_{n_3} \frac{1}{z_0^{-1} e^{\frac{\epsilon_{n_1 n_2 n_3}}{k_B T_{c,L}} - 1}} = n. \quad (9)$$

Note that the most significant difference among different boundary conditions is the difference in the ranges in Equation (9), in which the quantum numbers (n_1, n_2, n_3) vary. Particularly, the ground state energy which depends sensitively on α needs to be excluded during the calculation. For clarity, here we define $\alpha = k\pi$ ($k \in [0, 2]$).

- (i) $k \in [0, 1)$, the ground state $(0, 0, 0)$ should be excluded.
- (ii) $k \in (1, 2]$, the ground state $(-1, -1, -1)$ should be excluded.
- (iii) $k = 1$, the ground state $(-1, -1, -1)$, $(-1, -1, 0)$, $(-1, 0, -1)$, $(0, -1, -1)$, $(0, 0, -1)$, $(0, -1, 0)$, $(-1, 0, 0)$, $(0, 0, 0)$ should be excluded.

Obviously, the BEC statistics in the finite volume system not only depends on the linear size but also on the boundary conditions. We do some detailed calculations in following sections.

3. Finite-Size Effects on Bose–Einstein Condensation in the Cubic Box

In this section, performing the BEC statistics for the finite system of ideal Bose gases in the box traps of different linear sizes under periodic, antiperiodic, and Dirichlet boundary conditions, we compare their statistics and conclude on the finite-size effects on them.

(a) Periodic boundary condition ($\alpha = 0$)

According to our analyses, the discontinuous energy values of single-state can be given by:

$$\epsilon_{n_1 n_2 n_3} = \frac{2\hbar^2 \pi^2 (n_1^2 + n_2^2 + n_3^2)}{mL^2}. \quad (10)$$

The characteristic temperature can be determined by:

$$\frac{1}{L^3} \sum_{n_1} \sum_{n_2} \sum_{n_3} \frac{1}{e^{\frac{2\hbar^2\pi^2(n_1^2+n_2^2+n_3^2)}{mL^2k_B T_{c,L}}}-1} = n. \tag{11}$$

The numerical results under the periodic boundary condition are shown in Figures 1 and 2 and Table 1.

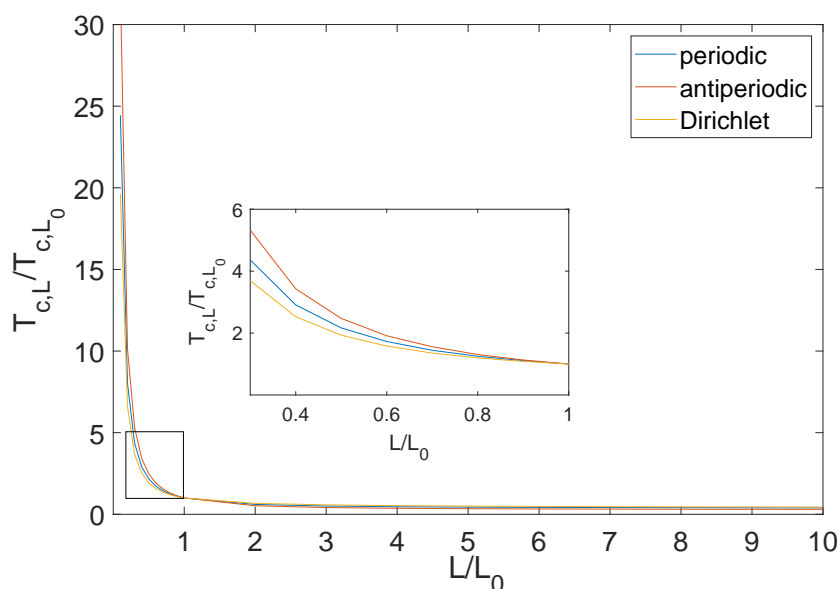


Figure 1. (Color online) The characteristic temperature $T_{c,L}$ versus L for an ideal Bose gases enclosed in the cubic box under the periodic, antiperiodic, and Dirichlet boundary conditions. L_0 is the unit length and T_{c,L_0} is the corresponding characteristic temperature.

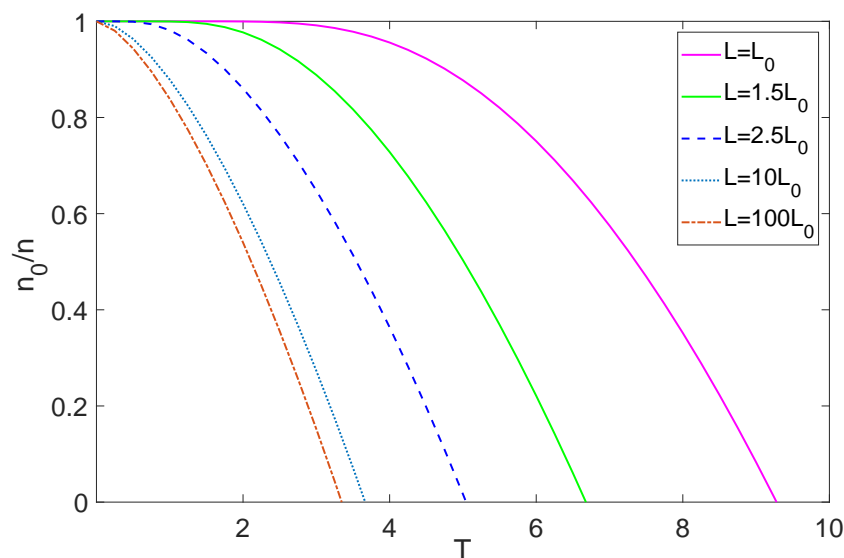


Figure 2. (Color online) The ground state particle density n_0/n versus T in the cubic box, with $L = L_0, 1.5L_0, 2.5L_0, 10L_0, 100L_0$, under the periodic boundary condition. Here, $\frac{\hbar^2}{mk_B} n^{\frac{2}{3}}$ is taken as a unit of T .

(b) Antiperiodic boundary condition ($\alpha = \pi$)

The quantum state energy is given by:

$$\epsilon_{n_1 n_2 n_3} = \frac{\hbar^2 [(2n_1\pi + \pi)^2 + (2n_2\pi + \pi)^2 + (2n_3\pi + \pi)^2]}{2mL^2}. \tag{12}$$

As a result, the characteristic temperature can be calculated by:

$$\frac{1}{L^3} \sum_{n_1} \sum_{n_2} \sum_{n_3} \frac{1}{e^{\frac{\hbar^2 \pi^2 [(2n_1+1)^2 + (2n_2+1)^2 + (2n_3+1)^2 - 3]}{2mL^2 k_B T_{c,L}}} - 1} = n. \tag{13}$$

Similarly, the corresponding results are shown in Figures 1 and 3 and Table 1.

(c) Dirichlet condition

This can be described by requiring that the wave function of the particle is identically zero outside the box. Hence, an impenetrable barrier can be interpreted as a boundary condition. The Dirichlet condition requires $\psi = 0$ on each side of the cubic box, $\psi_k(\frac{L}{2}) = \psi_k(-\frac{L}{2}) = 0$ ($k = x, y, z$). In this case, the single-state energy is:

$$\epsilon_{n_1 n_2 n_3} = \frac{\hbar^2 \pi^2 (n_1^2 + n_2^2 + n_3^2)}{2mL^2}. \tag{14}$$

The characteristic temperature can be derived by:

$$\frac{1}{L^3} \sum_{n_1=1}^{\infty} \sum_{n_2=1}^{\infty} \sum_{n_3=1}^{\infty} \frac{1}{e^{\frac{\hbar^2 \pi^2 (n_1^2 + n_2^2 + n_3^2 - 3)}{2mL^2 k_B T_{c,L}}} - 1} = n. \tag{15}$$

Here, note that the ranges of the quantum numbers (n_1, n_2, n_3) under Dirichlet boundary condition are from 1 to ∞ . Therefore, the nonvanishing ground state $(1, 1, 1)$, $\epsilon_0 = \frac{3\hbar^2 \pi^2}{2mL^2}$ should be excluded. Figures 1 and 4 and Table 1 depict the corresponding results.

Table 1. The characteristic temperature $T_{c,L}$ versus L for an ideal Bose gases enclosed in the cubic box of $L = 0.2L_0, 0.5L_0, 10L_0, 50L_0, 100L_0$, under the periodic, antiperiodic, and Dirichlet boundary conditions.

L/L_0	0.2	0.5	1	10	50	100
(a) $k_B T_{c,L} (\frac{\hbar^2}{m} n^{\frac{2}{3}})$	74.5	20.1	9.279	3.67	3.38	3.35
(b) $k_B T_{c,L} (\frac{\hbar^2}{m} n^{\frac{2}{3}})$	123.3	30	12.13	3.68	3.37	3.34
(c) $k_B T_{c,L} (\frac{\hbar^2}{m} n^{\frac{2}{3}})$	62.4	18.2	9.42	4.168	3.57	3.463

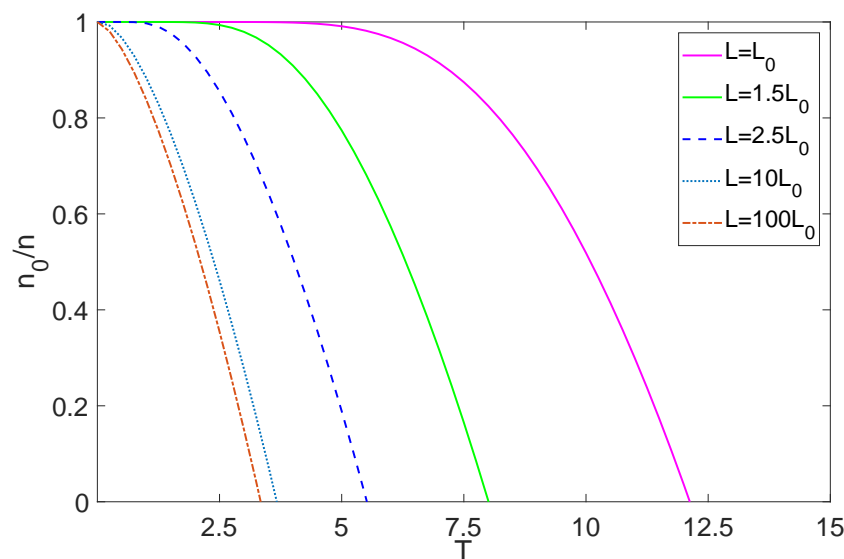


Figure 3. (Color online) The ground state particle density n_0/n versus T in the cubic box, with $L = L_0, 1.5L_0, 2.5L_0, 10L_0, 100L_0$, under the counter-periodic boundary condition. Here, $\frac{\hbar^2}{mk_B} n^{\frac{2}{3}}$ is taken as a unit of T .

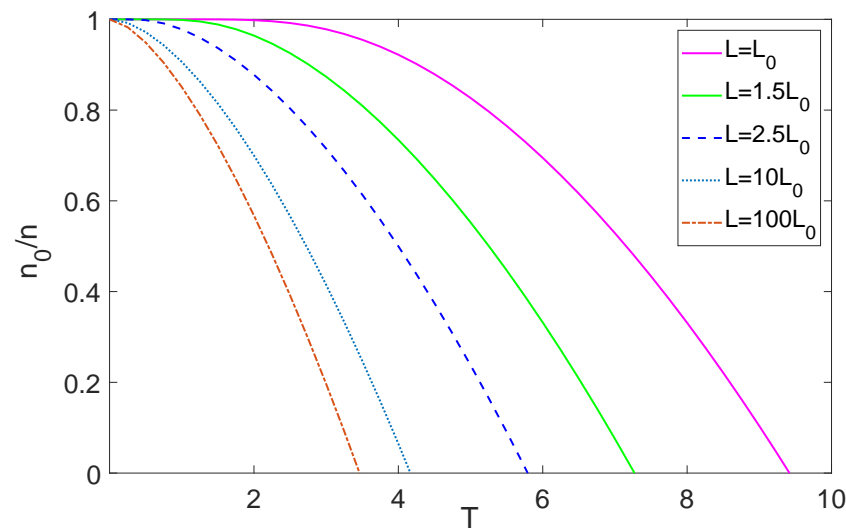


Figure 4. (Color online) The ground state particle density n_0/n versus T in the cubic box, with $L = L_0, 1.5L_0, 2.5L_0, 10L_0, 100L_0$, under the Dirichlet boundary condition. Here, $\frac{\hbar^2}{mk_B} n^{2/3}$ is taken as a unit of T .

By calculating numerically, the changes of $T_{c,L}$ with L , under periodic, antiperiodic, and Dirichlet conditions are shown in Figure 1. It is easy to check that, no matter which boundary condition is taken, at a fixed particle number density, $T_{c,L}$ considerably increases as L decreases in the region $L/L_0 < 1$. Since $T_{c,L}$ describes an approach to condensed state from the non-condensed one, the smaller linear size allows BEC to occur at higher temperature. When $L > 10L_0$, the values of $T_{c,L}$ agree with the results obtained within the thermodynamic limit results [35], as shown in Table 1, where we choose $\frac{\hbar^2}{mk_B} n^{2/3}$ as the $T_{c,L}$ unit. To illustrate this clearly, we numerically discuss the particle density for the ground state n_0 under the three boundary conditions sketched in Figures 2–4, respectively. It is clear that, as the linear size decreases the slope of the curves gradually becomes slower, condensate fraction n_0/n appears to increase. Namely, the smaller linear size is effective to increase the condensate fraction. Meanwhile, the intersection point of the curve and the horizontal axis $T_{c,L}$, being shifted to high value. The behavior further illustrates that $T_{c,L}$ describes the crossover behavior between ground and excited states, and $T_{c,L}$ becomes the critical temperature T_c when the volume of the system tend to infinity. These results are due to the fact that the coupling between energy level and linear size as Equation (9) can significantly alter the nature of BEC in the finite system. The smaller linear size can produce a stronger restrictions, and accordingly lower the mean energy, which can greatly facilitate the realization of BEC [46], increasing $T_{c,L}$ and n_0/n .

Consequently, the finite-size effects play an important role in the small volume systems, allowing for L -dependence of the shift of $T_{c,L}$ and n_0/n . The smaller is the linear size (the larger is the confinement), the higher is the $T_{c,L}$ and the greater is the n_0/n .

4. The Influences of Boundary Conditions on Bose–Einstein Condensation in a Cubic Box

To study the influence of α on condensation under twisted boundary conditions, we numerically calculate $T_{c,L}$ and n_0/n versus with α in the cases of $L = L_0$, $L = 10L_0$, and $L = 100L_0$, respectively. The numerical results are plotted in Figures 5–10, respectively.

As shown in Figures 5–7, obviously, in the interval $[0, 2\pi]$, the change of $T_{c,L}$ with α is symmetric about $\alpha = \pi$, which can be derived from Section 2. In the interval $[0, \pi]$, $T_{c,L}$ gradually becomes lower, but, when α reaches π , $T_{c,L}$ takes the maximum. This singular behavior is due to a significant fact that changes in boundary conditions disproportionately adds or removes single-states with the zero quantum numbers [47], and the contribution from that group of single-state to the non-condensed occupation is quite large. Compared with other boundary conditions, the antiperiodic boundary conditions remove more single-state with the zero quantum numbers, which can be derived in Section 2. As a result, the

fixed particle number density determines that the characteristic temperature $T_{c,L}$ takes its maximum at $\alpha = \pi$. Additionally, comparing Figures 5–7, as L increases until it is large enough, the influence of the boundary conditions on $T_{c,L}$ becomes negligible.

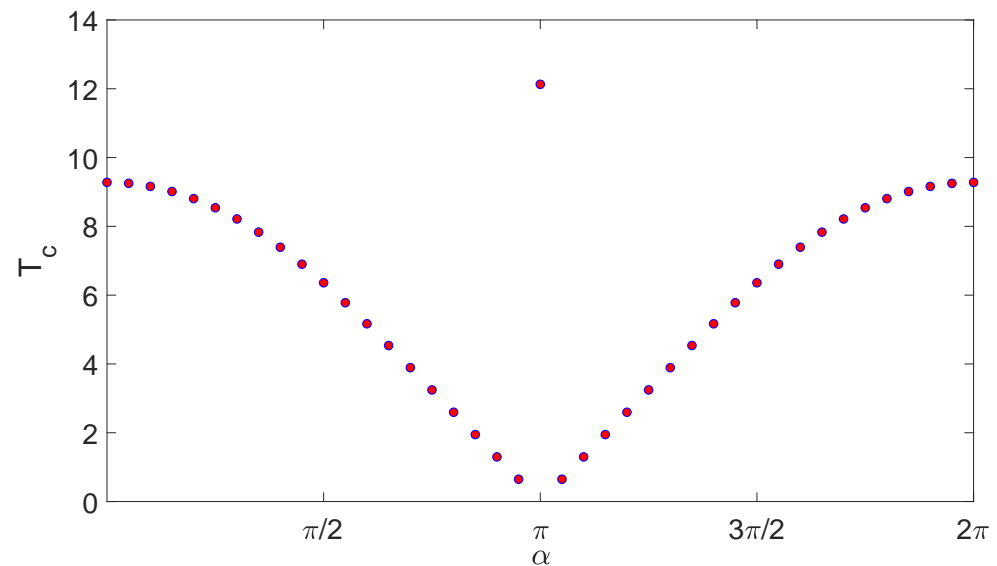


Figure 5. (Color online) The characteristic temperature $T_{c,L}$ versus α with $L = L_0$ in the cubic box. Here, $\frac{\hbar^2}{mk}n^{\frac{2}{3}}$ is taken as a unit of $T_{c,L}$.

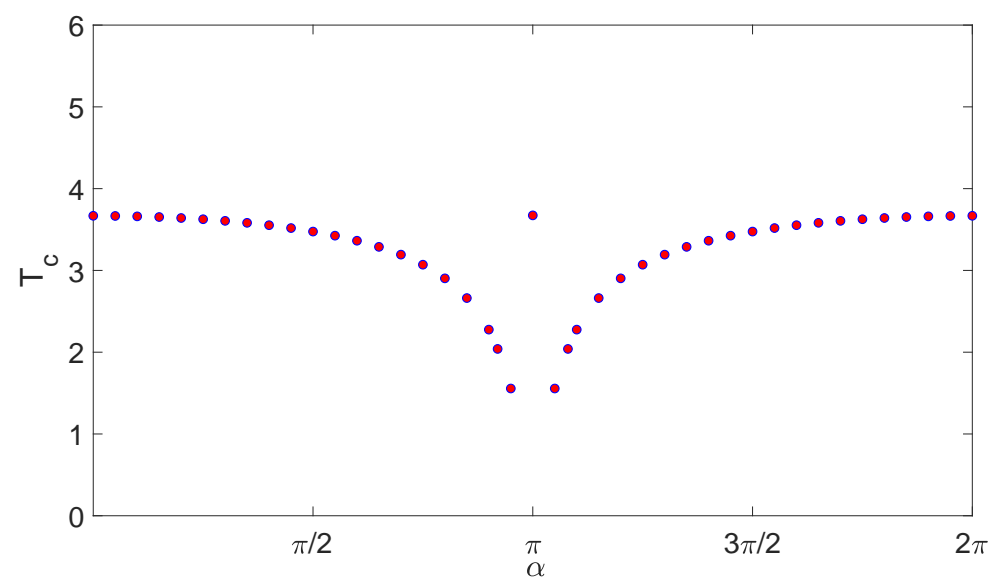


Figure 6. (Color online) The characteristic temperature $T_{c,L}$ versus α with $L = 10L_0$ in the cubic box. Here, $\frac{\hbar^2}{mk}n^{\frac{2}{3}}$ is taken as a unit of $T_{c,L}$.

Apart from this, the condensate fraction n_0/n versus T with various α in different linear sizes are presented in Figures 8–10. The condensate fraction become less sensitive to the boundary conditions as L increases. Particularly, Figure 10 demonstrates that the signature of BEC in finite systems become independent of the boundary conditions when the linear size is large enough. In the case of small volume systems, as α changes from 0 to π , the major difference is a retarded onset of the occupation of the ground state, while, at $\alpha = \pi$, the antiperiodic boundary condition is more conducive for bosons to condensation.

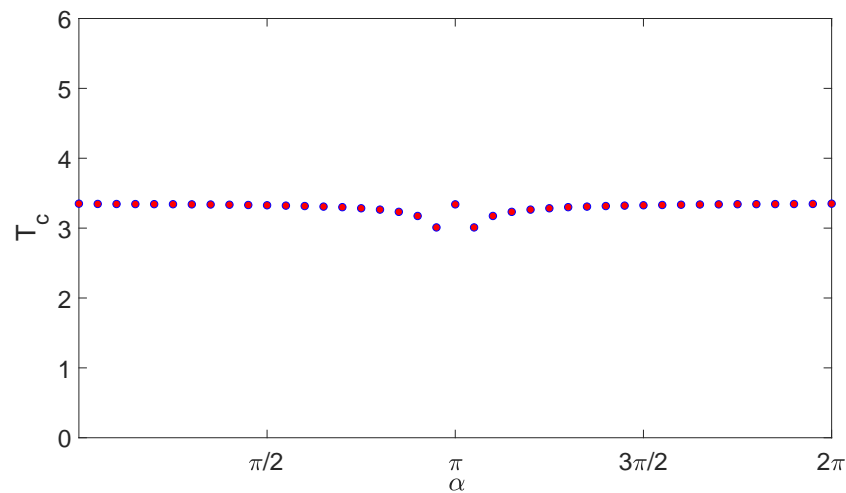


Figure 7. (Color online) The characteristic temperature $T_{c,L}$ versus α with $L = 100L_0$ in the cubic box. Here, $\frac{\hbar^2}{mk}n^{2/3}$ is taken as a unit of $T_{c,L}$.

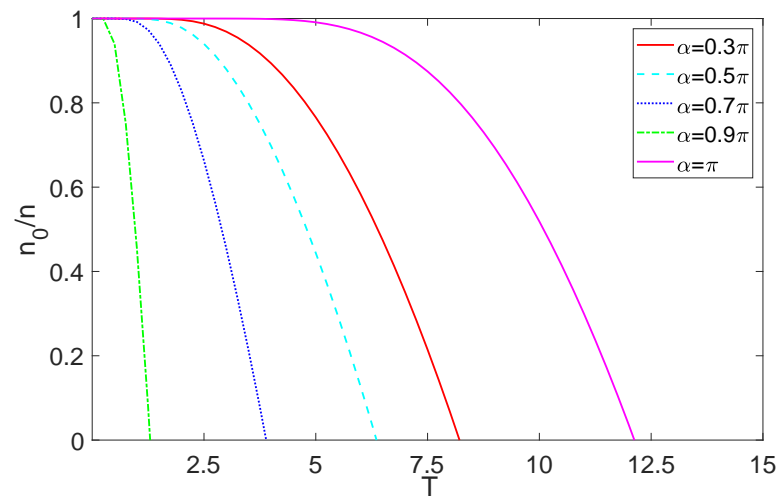


Figure 8. (Color online) The ground state particle density n_0/n versus T with $L = L_0$, with $\alpha = 0.3\pi, 0.5\pi, 0.7\pi, 0.9\pi, \pi$ in the cubic box. Here, $\frac{\hbar^2}{mk}n^{2/3}$ is taken as a unit of T .

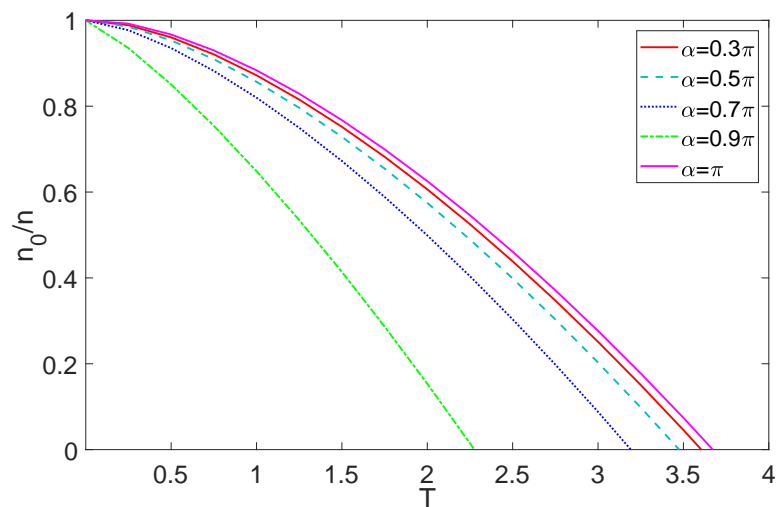


Figure 9. (Color online) The ground state particle density n_0/n versus T with $L = 10L_0$, with $\alpha = 0.3\pi, 0.5\pi, 0.7\pi, 0.9\pi, \pi$ in the cubic box. Here, $\frac{\hbar^2}{mk}n^{2/3}$ is taken as a unit of T .

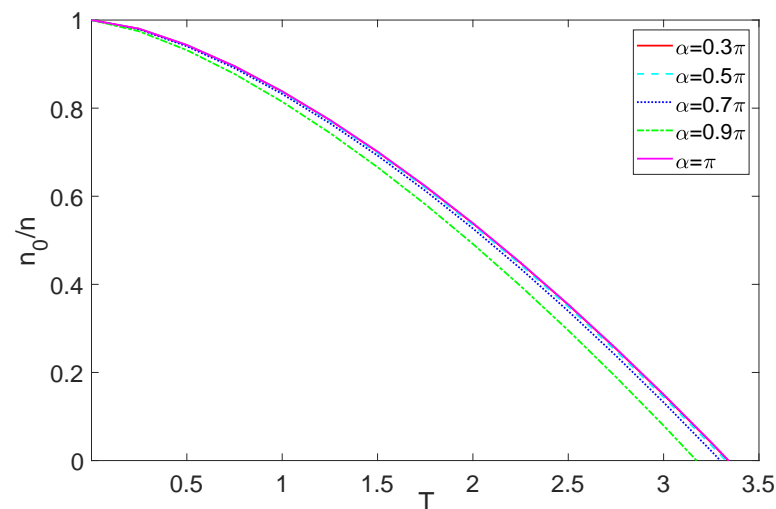


Figure 10. (Color online) The ground state particle density n_0/n versus T with $L = 100L_0$, with $\alpha = 0.3\pi, 0.5\pi, 0.7\pi, 0.9\pi, \pi$ in the cubic box. Here, $\frac{\hbar^2}{mk}n^{\frac{2}{3}}$ is taken as a unit of T .

As a consequence, in a system of small volume, the characteristic temperature and condensate fraction are sensitive to boundary conditions, especially in the case of antiperiodic boundary condition.

5. Conclusions

In this paper, we study ideal Bose gases with fixed particle density confined in the cubic box. By means of the theoretical analyses, we derive the specific formulas of the Bose distribution confined in the cubic box. Through numerical calculation, we analyze the influence of the finite-size and boundary conditions on characteristic temperature $T_{c,L}$ and condensate fraction n_0/n . We find that, in the case of finite volume system, the smaller linear size can increase $T_{c,L}$ and n_0 and the crossover behavior between the ground and excited states will advance as the linear size decreases. More importantly, the smaller is the volume, the more are sensitive $T_{c,L}$ and n_0/n to antiperiodic boundary conditions.

Additionally, superconductivity and superfluidity that have a lot in common with BEC can be described by similar theories. Therefore, the finite size effect is expected to have an important impact on superconductivity and superfluidity, which requires further research.

Author Contributions: Formal analysis, R.C.; Funding acquisition, Y.-L.W.; Methodology, R.C.; Resources, Q.-Y.W.; and Supervision, H.-S.Z. All authors have read and agreed to the published version of the manuscript.

Funding: This work was jointly supported by the National Nature Science Foundation of China (Grants Nos. 12075117, 51721001, 11890702, 11625418, 11535005, and 11690030) and the National Major state Basic Research and Development of China (Grant No. 2016YFE0129300). Y.-L.W. was funded by the Natural Science Foundation of Shandong Province of China (Grant No. ZR2020MA091).

Institutional Review Board Statement: Not applicable.

Informed Consent Statement: Not applicable.

Data Availability Statement: Not applicable.

Conflicts of Interest: The authors declare no conflict of interest.

References

1. Cataliotti, F.S.; Burger, S.; Fort, C.; Maddaloni, P.; Minardi, F.; Trombettoni, A.; Smerzi, A.; Inguscio, M. Josephson Junction Arrays with Bose-Einstein Condensates. *Science* **2001**, *293*, 843. [[CrossRef](#)] [[PubMed](#)]
2. Inguscio, M.; Stringari, S.; Bassani, F.; Liedl, G.L.; Wyder, P. Bose-Einstein Condensation. In *Encyclopedia of Condensed Matter Physics*; Elsevier: Oxford, UK, 2005; pp. 131–141.

3. Roati, G.; D'Errico, C.; Fallani, L.; Fattori, M.; Fort, C.; Zaccanti, M.; Modugno, G.; Modugno, M.; Inguscio, M. Anderson localization of a non-interacting Bose-Einstein condensate. *Nature* **2008**, *453*, 895. [[CrossRef](#)]
4. Wu, C.J.; Mondragon-Shem, I.; Zhou, X.F. Unconventional Bose—Einstein Condensations from Spin-Orbit Coupling. *Chin. Phys. Lett.* **2011**, *28*, 097102. [[CrossRef](#)]
5. Adhikari, S. Vortex-lattice in a uniform Bose-Einstein condensate in a box trap. *J. Phys. Cond. Matter.* **2019**, *31*, 275401. [[CrossRef](#)]
6. Deuchert, A.; Seiringer, R.; Yngvason, J. Bose-Einstein Condensation in a Dilute, Trapped Gas at Positive Temperature. *Commun. Math. Phys.* **2019**, *368*, 723–776. [[CrossRef](#)]
7. Urvoy, A.; Vendeiro, Z.; Ramette, J.; Adiyatullin, A.; Vuletić, V. Direct Laser Cooling to Bose-Einstein Condensation in a Dipole Trap. *Phys. Rev. Lett.* **2019**, *122*, 203202. [[CrossRef](#)]
8. Schneider, M.; Brächer, T.; Breitbach, D.; Lauer, V.; Pirro, P.; Bozhko, D.A.; Musiienko-Shmarova, H.Y.; Heinz, B.; Wang, Q.; Meyer, T. Bose-Einstein condensation of quasiparticles by rapid cooling. *Nat. Nanotechnol.* **2020**, *15*, 457–461. [[CrossRef](#)]
9. Georgescu, I. 25 years of BEC. *Nat. Rev. Phys.* **2020**, *2*, 396. [[CrossRef](#)]
10. Klaers, J.; Schmitt, J.; Vewinger, F.; Weitz, M. Bose-Einstein condensation of photons in an optical microcavity. *Nature* **2010**, *468*, 545–548. [[CrossRef](#)]
11. Hansen, A.; Schultz, J.T.; Bigelow, N.P. Singular atom optics with spinor Bose-Einstein condensates. *Optica* **2016**, *3*, 355–361. [[CrossRef](#)]
12. Goldstein, E.V.; Meystre, P. Quasiparticle instabilities in multicomponent atomic condensates. *Phys. Rev. A* **1997**, *55*, 2935–2940. [[CrossRef](#)]
13. Jochim, S.; Bartenstein, M.; Altmeyer, A.; Hendl, G.; Riedl, S.; Chin, C.; Hecker Denschlag, J.; Grimm, R. Bose-Einstein Condensation of Molecules. *Science* **2003**, *302*, 2101. [[CrossRef](#)]
14. Zwierlein, M.; Stan, C.; Schunck, C.; Raupach, S.; Gupta, S.; Hadzibabic, Z.; Ketterle, W. Observation of Bose-Einstein Condensation of Molecules. *Phys. Rev. Lett.* **2003**, *91*, 250401. [[CrossRef](#)] [[PubMed](#)]
15. Zhang, Z.; Chen, L.; Yao, K.; Chin, C. Atomic Bose-Einstein condensate to molecular Bose-Einstein condensate transition. *arXiv* **2020**, arXiv:2006.15297.
16. Anderson, M.H.; Ensher, J.R.; Matthews, M.R.; Wieman, C.E.; Cornell, E.A. Observation of Bose-Einstein Condensation in a Dilute Atomic Vapor. *Science* **1995**, *269*, 198. [[CrossRef](#)] [[PubMed](#)]
17. Davis, K.B.; Mewes, M.O.; Joffe, M.A.; Andrews, M.R.; Ketterle, W. Evaporative Cooling of Sodium Atoms. *Phys. Rev. Lett.* **1995**, *74*, 5202–5205. [[CrossRef](#)] [[PubMed](#)]
18. Ketterle, W.; Van Druten, N.J. Bose-Einstein condensation of a finite number of particles trapped in one or three dimensions. *Phys. Rev. A* **1996**, *54*, 656. [[CrossRef](#)]
19. Bradley, C.; Sackett, C.; Hulet, R. Bose-Einstein Condensation of Lithium: Observation of Limited Condensate Number. *Phys. Rev. Lett.* **1997**, *78*, 985–989. [[CrossRef](#)]
20. Brankov, J.; Dantchev, D.; Tonchev, N. *Theory of Critical Phenomena in Finite-Size Systems: Scaling and Quantum Effects*; World Scientific: Singapore, 2000.
21. Kristensen, M.; Christensen, M.; Gajdacz, M.; Iglicki, M.; Pawłowski, K.; Klempt, C.; Sherson, J.F.; Rzążewski, K.; Hilliard, A.J.; Arlt, J.J. Observation of Atom Number Fluctuations in a Bose-Einstein Condensate. *Phys. Rev. Lett.* **2019**, *122*, 163601. [[CrossRef](#)] [[PubMed](#)]
22. Andrews, M.; Townsend, C.; Miesner, H.J.; Durfee, D.; Kurn, D.; Ketterle, W. Observation of Interference between Two Bose Condensates. *Science* **1997**, *275*, 637. [[CrossRef](#)]
23. Myatt, C.; Burt, E.; Ghrist, R.; Cornell, E.; Wieman, C. Production of Two Overlapping Bose-Einstein Condensates by Sympathetic Cooling. *Phys. Rev. Lett.* **1997**, *78*, 586–589. [[CrossRef](#)]
24. Hall, D.S.; Matthews, M.R.; Ensher, J.R.; Wieman, C.E.; Cornell, E.A. Dynamics of Component Separation in a Binary Mixture of Bose-Einstein Condensates. *Phys. Rev. Lett.* **1998**, *81*, 1539–1542. [[CrossRef](#)]
25. Miesner, H.J.; Stamper-Kurn, D.; Stenger, J.; Inouye, S.; Chikkatur, A.; Ketterle, W. Observation of Metastable States in Spinor Bose-Einstein Condensates. *Phys. Rev. Lett.* **1999**, *82*, 2228–2231. [[CrossRef](#)]
26. Matthews, M.; Anderson, B.; Haljan, P.; Hall, D.; Wieman, C.; Cornell, E. Vortices in a Bose-Einstein Condensate. *Phys. Rev. Lett.* **1999**, *83*, 2498–2501. [[CrossRef](#)]
27. Papp, S.B.; Pino, J.M.; Wieman, C.E. Tunable Miscibility in a Dual-Species Bose-Einstein Condensate. *Phys. Rev. Lett.* **2008**, *101*, 040402. [[CrossRef](#)]
28. McCarron, D.; Cho, H.; Jenkin, D.; Köppinger, M.; Cornish, S. Dual-species Bose-Einstein condensate of ^{87}Rb and ^{133}Cs . *Phys. Rev. A* **2011**, *84*, 011603. [[CrossRef](#)]
29. Grossmann, S.; Holthaus, M. Bose-Einstein condensation in a cavity. *Z. Phys. B Condens. Matter* **1995**, *97*, 319–326. [[CrossRef](#)]
30. Ziff, R.M.; Uhlenbeck, G.E.; Kac, M. The ideal Bose-Einstein gas, revisited. *Phys. Rep.* **1977**, *32*, 169–248. [[CrossRef](#)]
31. Franzosi, R.; Giampaolo, S.M.; Illuminati, F. Quantum localization and bound-state formation in Bose-Einstein condensates. *Phys. Rev. A* **2010**, *82*, 063620. [[CrossRef](#)]
32. London, F. On the Bose-Einstein Condensation. *Phys. Rev.* **1938**, *54*, 947–954. [[CrossRef](#)]
33. Krueger, D.A. Finite Geometries and Ideal Bose Gases. *Phys. Rep.* **1968**, *172*, 211–223. [[CrossRef](#)]
34. Greenspoon, S.; Pathria, R.K. Bose-Einstein condensation in finite noninteracting systems: A new law of corresponding states. *Phys. Rev. A* **1974**, *9*, 2103. [[CrossRef](#)]

35. Holthaus, M.; Kapale, K.T.; Scully, M.O. Influence of boundary conditions on statistical properties of ideal Bose-Einstein condensates. *Phys. Rev. E* **2002**, *65*, 036129. [[CrossRef](#)]
36. Brankov, J.G.; Danchev, D.M.; Tonchev, N.S. *Theory of Critical Phenomena in Finite-Size Systems*; World Scientific: Singapore, 2020; Volume 9, p. 460. [[CrossRef](#)]
37. Byers, N.; Yang, C.N. Theoretical Considerations Concerning Quantized Magnetic Flux in Superconducting Cylinders. *Phys. Rev. Lett.* **1961**, *7*, 46–49. [[CrossRef](#)]
38. Zawadzki, K.; D’Amico, I.; Oliveira, L.N. Symmetries and Boundary Conditions with a Twist. *Braz. J. Phys.* **2017**, *47*, 488–511. [[CrossRef](#)]
39. Sachrajda, C.T.; Villadoro, G. Twisted boundary conditions in lattice simulations. *Phys. Lett. B* **2005**, *609*, 73–85. [[CrossRef](#)]
40. Könenberg, M.; Moser, T.; Seiringer, R.; Yngvason, J. Superfluid behavior of a Bose-Einstein condensate in a random potential. *New J. Phys.* **2015**, *17*, 013022. [[CrossRef](#)]
41. Könenberg, M.; Moser, T.; Seiringer, R.; Yngvason, J. Superfluidity and BEC in a Model of Interacting Bosons in a Random Potential. *J. Phys. Conf. Ser.* **2016**, *691*, 012016. [[CrossRef](#)]
42. Kleman, M.; Friedel, J. Disclinations, dislocations, and continuous defects: A reappraisal. *Rev. Mod. Phys.* **2008**, *80*, 61–115. [[CrossRef](#)]
43. Karbowski, J.; Turski, L. The Bose-Einstein condensation in random box. *Phys. A* **2000**, *276*, 489–494. [[CrossRef](#)]
44. Dalfovo, F.; Pitaevskii, L.; Stringari, S. Bose Einstein Condensates. *Uspekhi Fiz. Nauk.* **2005**, *167*. [[CrossRef](#)]
45. Kirsten, K.; Toms, D.J. Bose-Einstein condensation under external conditions. *Phys. Lett. A* **1998**, *243*, 137–141. [[CrossRef](#)]
46. Bagnato, V.; Pritchard, D.E.; Kleppner, D. Bose-Einstein condensation in an external potential. *Phys. Rev. A* **1987**, *35*, 4354–4358. [[CrossRef](#)] [[PubMed](#)]
47. Tarasov, S.; Kocharovskiy, V.; Kocharovskiy, V. Anomalous Statistics of Bose-Einstein Condensate in an Interacting Gas: An Effect of the Trap’s Form and Boundary Conditions in the Thermodynamic Limit. *Entropy* **2018**, *20*, 153. [[CrossRef](#)] [[PubMed](#)]